


# Increased Risk of Extreme Precipitation Over an Urban Agglomeration With Future Global Warming

**Journal Article****Author(s):**

Doan, Quang-Van; Chen, Fei; Kusaka, Hiroyuki; [Dipankar, Anurag](#) ; Khan, Ansar; Hamdi, Rafiq; Roth, Matthias; Niyogi, Dev

**Publication date:**

2022-06

**Permanent link:**

<https://doi.org/10.3929/ethz-b-000555980>

**Rights / license:**

[Creative Commons Attribution-NonCommercial-NoDerivatives 4.0 International](#)

**Originally published in:**

Earth's Future 10(6), <https://doi.org/10.1029/2021EF002563>

# Earth's Future



## RESEARCH ARTICLE

10.1029/2021EF002563

## Increased Risk of Extreme Precipitation Over an Urban Agglomeration With Future Global Warming

Quang-Van Doan<sup>1,2</sup> , Fei Chen<sup>2</sup> , Hiroyuki Kusaka<sup>1</sup>, Anurag Dipankar<sup>3</sup>, Ansar Khan<sup>4</sup> , Rafiq Hamdi<sup>5</sup>, Matthias Roth<sup>6</sup>, and Dev Niyogi<sup>7</sup> 

<sup>1</sup>Center for Computational Sciences, University of Tsukuba, Tsukuba, Japan, <sup>2</sup>Research Applications Laboratory, National Center for Atmospheric Research, Boulder, CO, USA, <sup>3</sup>Institute for Atmospheric and Climate Science, ETH, Zurich, Switzerland, <sup>4</sup>Department of Geography, Lalbaba College, University of Calcutta, Kolkata, India, <sup>5</sup>Royal Meteorological Institute of Belgium, Brussels, Belgium, <sup>6</sup>Department of Geography, National University of Singapore, Singapore, Singapore, <sup>7</sup>Jackson School of Geosciences, and Cockrell School of Engineering, University of Texas at Austin, Austin, TX, USA

### Key Points:

- New normal of “extreme events get more extreme” in future city-scale precipitation is revealed
- Global warming could modify and even reduce the urban footprint on extreme precipitation (EP) events
- The intensification of EP can reach the maximum at the “super” Clausius-Clapeyron ( $\geq +7\%$  per K warming) rate

### Supporting Information:

Supporting Information may be found in the online version of this article.

### Correspondence to:

Q.-V. Doan,  
doan.van.gb@u.tsukuba.ac.jp

### Citation:

Doan, Q.-V., Chen, F., Kusaka, H., Dipankar, A., Khan, A., Hamdi, R., et al. (2022). Increased risk of extreme precipitation over an urban agglomeration with future global warming. *Earth's Future*, 10, e2021EF002563. <https://doi.org/10.1029/2021EF002563>

Received 18 NOV 2021

Accepted 20 APR 2022

### Author Contributions:

**Conceptualization:** Quang-Van Doan, Fei Chen, Hiroyuki Kusaka, Anurag Dipankar, Ansar Khan, Rafiq Hamdi, Matthias Roth, Dev Niyogi

**Formal analysis:** Quang-Van Doan

**Investigation:** Quang-Van Doan, Fei Chen, Hiroyuki Kusaka, Anurag Dipankar, Ansar Khan, Rafiq Hamdi, Matthias Roth, Dev Niyogi

**Methodology:** Quang-Van Doan, Anurag Dipankar

**Software:** Quang-Van Doan

**Abstract** Understanding the response of extreme precipitation (EP) at a city scale to global warming is critical to reducing the respective risk of urban flooding. Yet, current knowledge on this issue is limited. Here, focusing on an urban agglomeration in the tropics, Singapore, we reveal that future global warming enhances both frequency and intensity of EP, based on simulations with a state-of-the-art convection-permitting regional climate model. EP intensification can reach maximum “super” Clausius-Clapeyron rate ( $\geq +7\%$  per K warming) rate, implying a “new normal” of “extreme events get more extreme,” which is consistently for both Representative Concentration Pathways 8.5 and 4.5. The intensification is lower for moderate and light precipitation. Also, global warming was found to dampen the urban effect on EP events. The EP enhancement is attributed to the increased atmospheric moisture and convective inhibition due to enhanced low-level stratification that delays a convection to develop until it becomes more intense.

**Plain Language Summary** Understanding the response of extreme precipitation (EP) at a city scale to global warming is critical to reducing the respective risk of urban flooding. Here we show that future global warming will enhance both frequency and intensity of EP, based on simulations with a state-of-the-art convection-permitting regional climate model for an urban agglomeration in the tropics, Singapore. EP is estimated to intensify much more than moderate and light precipitation, implying a “new normal” of “the extreme events get more extreme.” Also, global warming was found to dampen the urban effect on EP events. The EP enhancement is attributed to the increased atmospheric moisture and convective inhibition due to enhanced low-level stratification that delays a convection to develop until it becomes more intense.

## 1. Introduction

Recent decades have witnessed an increased occurrence of natural disasters, including floods associated with extreme precipitation (EP) in cities (IPCC AR6, 2022). Making cities safe, resilient, and sustainable is one of United Nations Sustainable Development Goals 2030 (SDG2030, especially Goal 11; United Nations, 2015). Achieving this goal is a challenge because cities are exposed to changing large-scale climatic feedbacks, and cities themselves are creating their microclimate. Such multiscale climatic forcing is causing non-stationarity in the climate system, which results in an increasing trend of unprecedented extreme weather and climate events that might occur in the future (Differbaugh et al., 2017; Fischer et al., 2021). As a result, urban areas that are designed based on historical hydroclimate conditions continue to be exposed to higher risk due to climate impacts, especially urban floods (Mishra et al., 2022; Ye & Niyogi, 2022). Indeed, it is recognized that for some regions, precipitation extremes will become more frequent, more widespread, and/or more intense during the 21st century, and cities will be disproportionately at higher risk (Meyer et al., 2020).

A basis of framing the precipitation change due to climate warming is through the classical Clausius-Clapeyron (CC) relation (Fowler, Lenderink, et al., 2021; Lenderink & van Meijgaard, 2009). The CC equation defines the saturation specific humidity of the atmosphere as a function of temperature. Hence, specific humidity near the Earth's surface is anticipated to rise at a rate of approximately 7% per degree warming ( $K^{-1}$ ). Several past studies have shown that both short- (<1 day) and long-duration (>1 day) precipitation extremes intensify at a rate consistent with the increase in atmospheric moisture ( $\sim 7\% K^{-1}$ ; Allan & Soden, 2008). In some regions,

© 2022. The Authors. Earth's Future published by Wiley Periodicals LLC on behalf of American Geophysical Union. This is an open access article under the terms of the [Creative Commons Attribution-NonCommercial-NoDerivs License](https://creativecommons.org/licenses/by/4.0/), which permits use and distribution in any medium, provided the original work is properly cited, the use is non-commercial and no modifications or adaptations are made.

**Validation:** Quang-Van Doan, Anurag Dipankar

**Visualization:** Quang-Van Doan, Ansar Khan

**Writing – original draft:** Quang-Van Doan

**Writing – review & editing:** Quang-Van Doan, Fei Chen, Hiroyuki Kusaka, Anurag Dipankar, Ansar Khan, Rafiq Hamdi, Matthias Roth, Dev Niyogi

however, the increase in short-duration extreme rainfall intensity shows a higher scaling than the CC relation, that is, “super” CC rate (Ali, Fowler, et al., 2021; Fischer & Knutti, 2016; Guerreiro et al., 2018; Rajczak & Schär, 2017; Scherrer et al., 2016; Westra et al., 2014). However, the mechanisms that lead to the “super” CC rate are not well understood, especially those that influence latent heat release, temperature stratification, and large-scale circulation dynamics (Fowler, Ali, et al., 2021). Uncertainties regarding the response of short-duration precipitation extremes to global warming and the relevant mechanisms were extensively addressed in previous literature (Berg et al., 2013; Deser et al., 2012; Lenderink & Meijgaard, 2010; Lenderink & van Meijgaard, 2009; Panthou et al., 2014; Park & Min, 2017; Shepherd, 2014).

Several past studies have pointed out the impact of global warming on heavy precipitation. However, only a few studies have explored the future changes in EP at small spatiotemporal scales (especially those at a city scale; Ali & Mishra, 2018; Ali, Peleg, & Fowler, 2021; Li et al., 2020; Moustakis et al., 2020; Wasko et al., 2016). This is due to limited data and computational resources required for conducting city-scale relevant meteorological simulations. Another reason relates to the large uncertainties involved in our understanding of processes at the city scale, which can influence short-term precipitation. Such uncertainties include socio-economic forecasts, greenhouse emission scenarios, global climate models (GCMs) errors, and lack of physical parameterization schemes representing complex urban thermodynamics processes. Also, due to its coarse resolution, a GCM is unable to explicitly represent convection processes, which is important for short-duration precipitation. Recent studies show that convection-permitting models substantially improve the simulation of local storms as the details of convection organization are better represented (e.g., Fowler, Ali, et al., 2021). Additionally, there are unique urban-scale processes which contribute to enhanced urban precipitation (Doan et al., 2021; Kishitawal et al., 2010; Kusaka et al., 2014; Niyogi et al., 2011; Singh et al., 2020; Wang et al., 2021; Yang et al., 2021). They include increased convection from urban heat island (UHI) effect, urban roughness (Shem & Shepherd, 2009), mesoscale circulations (land-sea breeze effect; Doan et al., 2021), differential aerosol loading between urban/surrounding natural land (Heever & Cotton, 2007), urban barrier effect (e.g., Bornstein et al., 1994). These factors are summarized in Liu and Niyogi (Liu & Niyogi, 2019). These processes can be explicitly modeled by state-of-the-art regional/urban-scale models with building parameterizations and urban metabolism (Hamdi et al., 2020).

Here, we assess the climatic response of EP at a city scale to global warming using Singapore as an example. The primary question of interest is: how will EP change in the future? More specifically, we address two research questions regarding city-scale EP change: (a) does the local EP show a significant global warming signal, and (b) what atmospheric processes are responsible for eventual EP changes? We employ a state-of-the-art convection-permitting regional climate model based on the Weather Research Forecasting (WRF) modeling system, whose performance to simulate EP is verified against in situ observed and satellite-derived rainfall products. Using dynamical downscaling, future EP climates until 2100 are simulated using Representative Concentration Pathways (RCPs) 8.5 and 4.5, respectively.

## 2. Materials and Methods

### 2.1. Model Configuration

A convection-permitting regional climate model, named Weather Research and Forecast (W. C. Skamarock et al., 2008; WRF), is used to simulate current-time and future precipitation climates over the Singapore region. The model is designed to have three nested domains with horizontal resolutions of  $30 \times 30$ ,  $6 \times 6$ , and  $2 \times 2$  km for gradually inheriting the large-scale atmospheric forcing while resolving the localized convective processes. The innermost domain, having the size of  $154 \times 154$  grid cells, covers the Singapore metropolitan area, the Southern Malaysia peninsula, and a part of the Indonesian islands (Figure S1 in Supporting Information S1). The physical schemes of WRF (shown in Table 1) are selected based on their widespread use in regional climate simulations. Note that the cumulus parameterization scheme is applied for the outermost domain only because fine resolutions of the inner domains allow them to resolve the convection processes explicitly. For modeling the urban effect, the single-layer urban canopy model (Kusaka & Kimura, 2004; Kusaka et al., 2001) is activated within the Noah land surface modeling (Chen et al., 2011) framework. To better represent the urban area, up-to-date urban land cover information (Demuzere et al., 2021) is used and overlaid over the default USGS land use database provided by WRF (Figure S2 in Supporting Information S1). Default urban parameters provided by WRF are used in the simulations. A few model tests with different physical schemes have been conducted and the results show that the variabilities in the precipitation simulations exist but are small compared to the impact of warming climate.

**Table 1**  
*Model Configuration and Physical Scheme Settings*

	Domain 01	Domain 02	Domain 03
Grid spacing	30.0 km	6.0 km	2.0 km
Number of grids	120 × 120	206 × 206	154 × 154
Number of vertical layers	35 layers		
Microphysics scheme	WRF single-moment 6-class scheme (Hong, 2006)		
Shortwave radiation	Dudhia Shortwave scheme (Dudhia, 1989)		
Longwave radiation	RRTM Longwave scheme (Mlawer et al., 1997)		
Boundary layer scheme	Yonsei university scheme (Hong et al., 2006)		
Land surface scheme	Noah land-surface model (Mukul Tewari et al., 2004)		
Urban canopy model	Single-layer urban canopy model (Kusaka et al., 2001)		
Cumulus	Kain-Fritsch scheme (Kain, 2004) (Domain 01 only)		

*Note.* WRF, Weather Research Forecasting.

## 2.2. Experimental Design

We conducted three separate simulations using different climate scenarios while keeping the same urban surface conditions (see Table 2 for climate scenarios) and two urban-effect sensitivity simulations. The first simulation, that is, the baseline climate (BC), reproduces the current climate. Two climate-change sensitivity simulations, that is, the future climate (FC), are aimed to dynamically downscale future climate under global warming up the end of the 21st century following two Representative Concentration Pathways (RCP) 8.5 and 4.5 (van Vuuren et al., 2011). Two urban-effect sensitivity simulations were conducted. The first is baseline climate simulation without urban land use/cover (LUC; i.e., urban LUC has been replaced by the cropland as the dominant LUC surrounding the urban surface over the region of interest). The simulation, hereafter, is called BCw/oU in contrast with BCw/U or BC, that is, the BC simulation with the “status-quo” urban LUC. The second is FC without urban LUC, hereafter called FCw/oU in contrast with FCw/U or FC, that is, the FC simulation with the “status-quo” urban LUC. Note that only one scenario RCP8.5 is used for the future climate simulation without urban LUC. In detail, ERA-Interim reanalysis data (Dee et al., 2011) is used as initial and boundary conditions (IBCs) and run for November 2005–2014. November is selected because it falls into the inter-monsoon period (between the Southwest and Northeast monsoon seasons) when the prevailing wind is relatively weak, and the wet atmosphere is dominantly characterized by localized thunderstorms (Doan et al., 2021; Fong & Ng, 2012; Simón-Moral et al., 2021). Such atmospheric conditions are believed to be the most suitable for this study, which focuses on city-scale processes, and urban effects are known to be more apparent on smaller scale precipitation than that caused by large-scale atmospheric circulations.

On the other hand, the FC simulations are forced by IBCs created using the pseudo-global warming (PGW) approach. PGW is a widely used dynamical downscaling method for investigating the response of localized weather to the global warming effect (Doan & Kusaka, 2018; Gutmann et al., 2018; Hibino et al., 2018; Lauer et al., 2013; Pall et al., 2017; Rasmussen et al., 2011; Sato et al., 2007; Schär et al., 1996). In PGW, RCMs are forced by “pseudo” future atmospheric conditions, defined as present-time reanalysis data augmented by

**Table 2**  
*List of Initial and Boundary Conditions Used for Simulations*

Experiments	Description	Initial & boundary conditions
BC	Baseline Climate	ERA Interim, Novembers 2005–2014
FC RCP8.5	Future climate up to 2080–2099 with scenario RCP8.5	CMIP5 RCP8.5 ensemble means (36 GCMs) GWI (2080–2099 minus 2000–2019) + ERA Interim, Novembers 2005–2014
FC RCP4.5	Future climate up to 2080–2099 with scenario RCP8.5	CMIP5 RCP8.5 ensemble means (30 GCMs) GWI (2080–2099 minus 2000–2019) + ERA Interim, Novembers 2005–2014

*Note.* GWI, global warming increment.

so-called global warming increments (GWIs; Doan & Kusaka, 2018). First, we calculate GWIs as anomalies between the future and current climate (in terms of monthly mean), provided by a GCM or ensemble of GCMs, for primary atmospheric variables, that is, surface and air temperature, geopotential, wind (two components). Note that the relative humidity of PGW data is kept the same as present-time reanalysis data. GWIs are then re-gridded and added to the reanalysis data of interest to be handled by RCMs. Details of the technical procedure of PGW as well as its advantages and disadvantages are well documented in previous literature (Doan & Kusaka, 2018; Rasmussen et al., 2011; Sato et al., 2007).

A reason for selecting the PGW dynamical downscaling is because the method can be used to isolate the primary signal of the global warming effect. PGW literally ignores the potential change in inter-annual and daily variabilities of the future climate system (Lauer et al., 2013; Sato et al., 2007). This characteristic allows us to focus exclusively on how a warming background climate modifies EP. The secondary impacts of global warming, such as the impacts of potential changes in weather variabilities, are intentionally not included in this study; such can be also considered as a limitation of our study.

In terms of technical details, GWIs in this study are calculated as anomalies between the future and the reference climate data provided by CMIP5 GCMs (Meehl et al., 2009; Taylor et al., 2012). The future climate is defined as November mean for 20 years 2080–2099; meanwhile, the reference climate is 2000–2019. Two emission scenarios, that is, RCP4.5 and RCP8.5, are selected for the sake of covering inter-scenario uncertainty. To reduce the GCM-related bias, the ensemble mean of multiple GCMs are used instead of a single GCM. In detail, 36 GCMs for RCP8.5 and 30 GCMs for RCP4.5 are used for calculating the mean. GWIs values are then re-gridded and added over 6-hourly ERA-Interim reanalysis data to generate IBCs for WRF.

### 2.3. Rainfall Data

In situ measurement rainfall data used to evaluate the model's performance are from five manned weather stations, named Changi, Paya Lebar, Seletar, Sembawang and Tengah (S-24, S-06, S-25, S-80, and S-23). These stations are managed by the Meteorological Service Singapore (MSS). Rainfall values are hourly totals (e.g., 01:00LT rainfall is backward accumulated between 00:01 and 01:00LT). A quality check is conducted in MSS by comparing against both tipping buckets and radar images ([http://www.weather.gov.sg/learn\\_observations/](http://www.weather.gov.sg/learn_observations/)). Observed data in November from 2005 to 2014 corresponding to the simulation period is used for model evaluation.

Satellite precipitation product—CMORPH (CPC MORPHing technique; NCEP, 2021) is used to complement in situ measurement for the model verification. CMORPH precipitation is derived from low orbiter satellite microwave observations exclusively and whose features are transported via spatial propagation information obtained entirely from geostationary satellite IR data. It has been bias corrected to form a global, high resolution precipitation analysis. Data used in this study have  $8 \times 8$  km spatial resolution with a temporal resolution of 30 min from January 1998 to the present.

## 3. Results and Discussions

The performance of WRF on regional precipitation and its extremes is evaluated against both in situ measurements and satellite-derived precipitation products (CMORPH). The model agrees well with observations regarding the probability distribution of hourly precipitation across almost all precipitation intensities (Figure 1a). The quantile-quantile (Q-Q) comparison provides a more specific comparison between the observed and modeled rainfall (Figure 1b). Overall, the model slightly underestimates measured precipitation, especially at very high quantiles. NOAA's satellite-derived NOAA CPC Morphing Technique (CMORPH) data (Joyce et al., 2004) is used to expand “observed” rainfall coverage. For direct comparison, the WRF output is upscaled to the resolution of the satellite product (to  $8 \times 8$  km). The agreement between the model and CMORPH is relatively more minor, with the model overestimating high precipitation quantiles (up to 80%) and underestimating low quantiles (Figures 1c and 1d). However, the overestimation of high precipitation quantiles is expected because of the relatively coarse resolution of the CMORPH product, which tends to smooth out fine-scale EP (NCEP, 2021). Considering this known absolute bias, the agreement in the diurnal cycle and spatial variation of rainfall between WRF and CMORPH is reasonable (Figure S3 in Supporting Information S1).

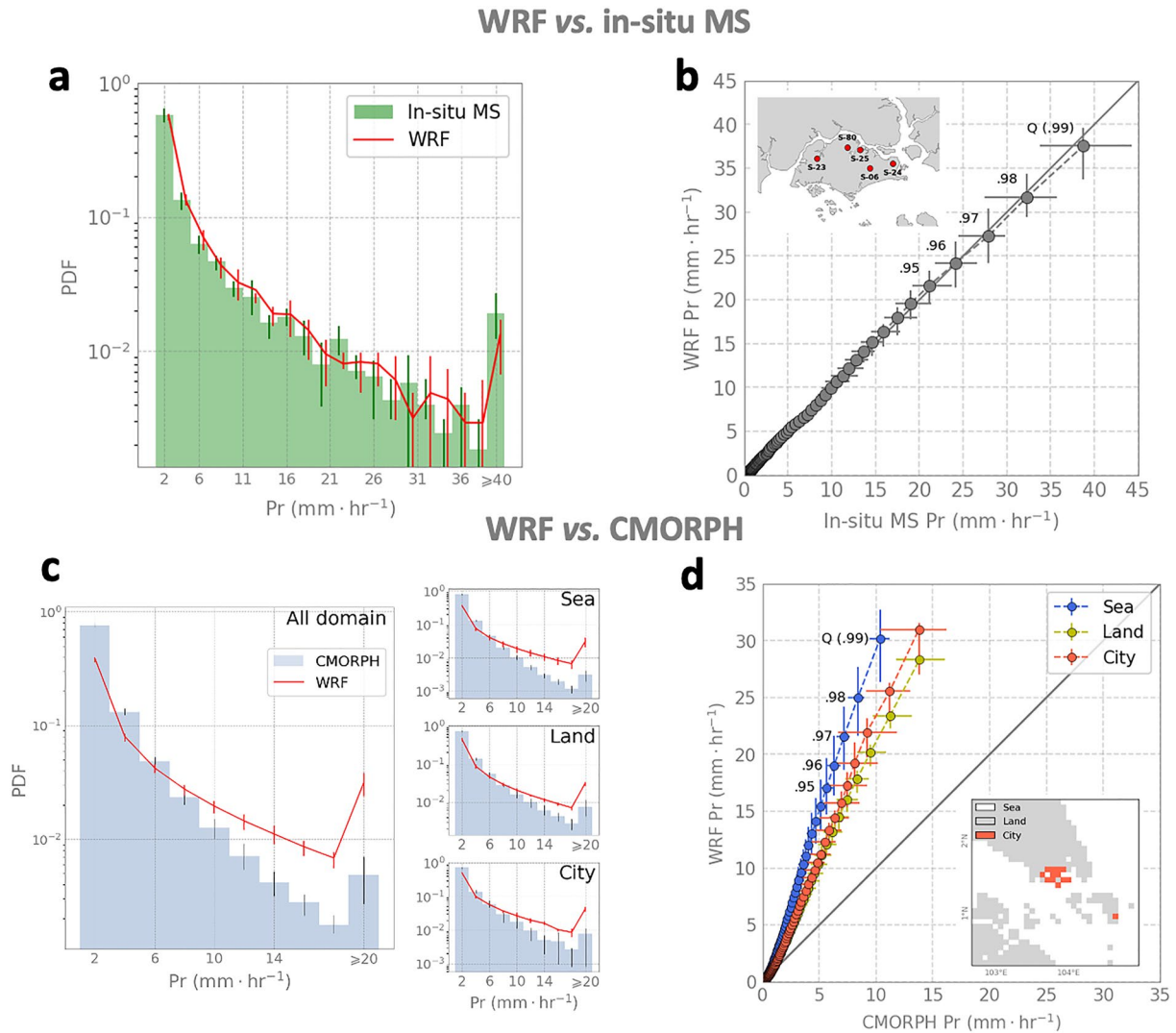


**Figure 1.** Weather Research and Forecast (WRF) performance against in situ measurement and satellite-derived precipitation product. (a) Probability density function (PDF) of WRF simulations and in situ measurements at six weather stations (see inset of b) run by the Meteorological Service Singapore. Results are averages across five stations of modeled (corresponding to the grid of the in situ locations) and observed hourly data in November for 10 years 2005–2014. (b) Quantile-quantile (Q-Q) plot for WRF and in situ measurement data. (c) PDF of WRF simulations and satellite-derived precipitation CMORPH analysis. Left panel is the average PDF of all grid cells in the domain of interest (inset map in d). WRF rainfall values are upscaled to match the spatial resolution of CMORPH data (approximately  $8 \times 8$  km). Right panels show PDFs for different surface covers, that is, sea, land, and city, respectively. (d) Q-Q plot for WRF and CMORPH rainfall. Uncertainty ranges shown in all panels indicate annual variability, that is, the range between percentile 25 and 75 of annual values (10 years).

### Extreme Events Get More Extreme

The question related to the future change is investigated by examining the difference between simulations for baseline climate (BC) and future climate (FC). Several interesting features stand out. First, the comparison shows a notable increase in the simulated EP in the future, namely an increase in event frequency and enhanced precipitation intensity (Figure 2). Second, the characteristics of the changes are different with different precipitation types, revealing a more significant increase for heavy precipitation compared to lighter precipitation. For example, the occurrence probability of precipitation under  $10 \text{ mm hr}^{-1}$  is projected to increase by 10% (under scenario RCP8.5). In contrast for precipitation greater than  $30 \text{ mm hr}^{-1}$ , the increase can reach 50% or greater (Figure 2a lower panel). The increasing trend is consistently seen for both RCP scenarios. However, the extent of the change is different between RCPs, smaller for RCP4.5 and larger for RCP8.5. Interestingly, there is almost no inter-scenario difference for light precipitation, which becomes more pronounced for heavier precipitation.

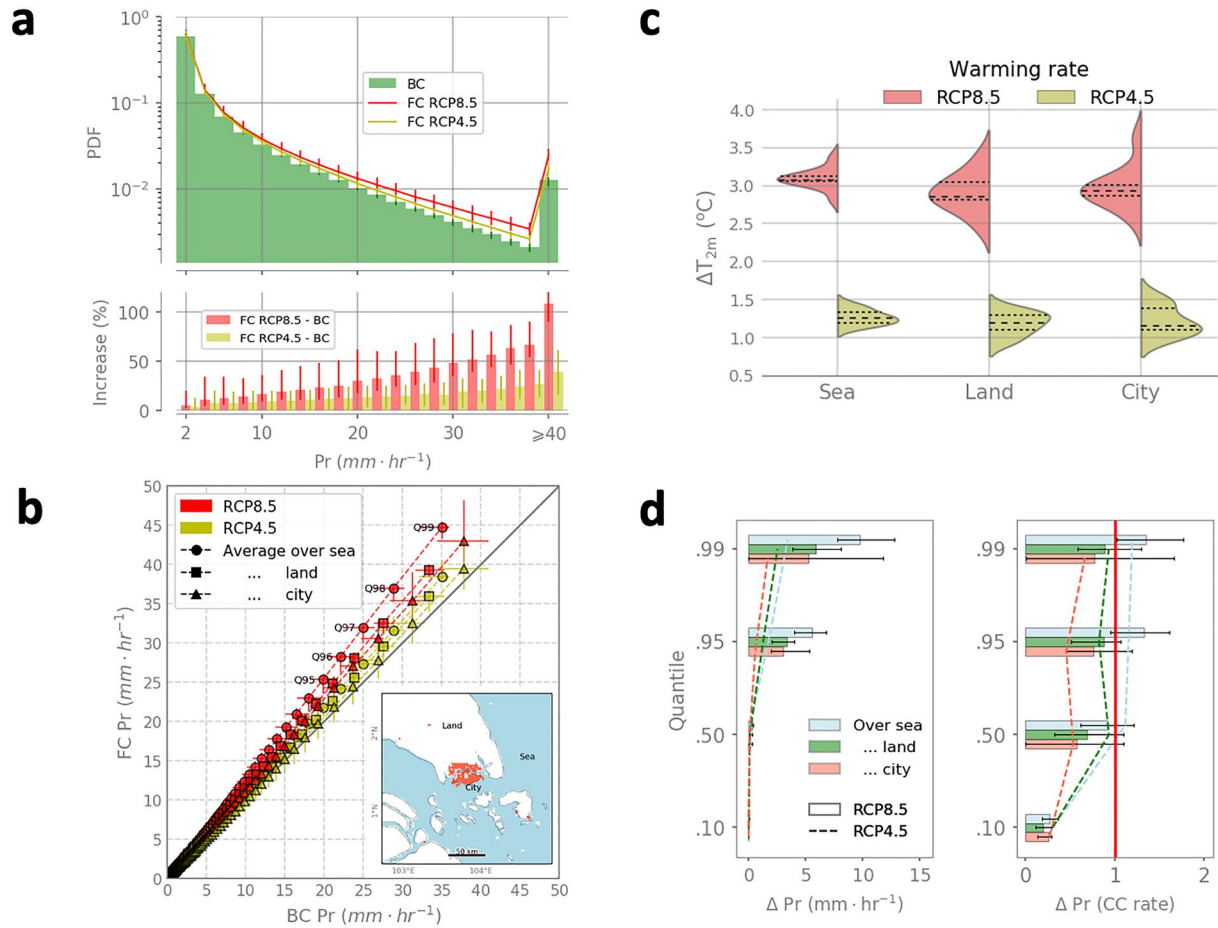


**Figure 2.** Extreme precipitation becomes more frequent and intense with global warming. (a) Probability density functions (PDFs) of baseline climate (BC) and future climate (FC) (upper sub-panel) and anomaly of FC relative to BC in percent (lower sub-panel). PDFs are whole-domain averages calculated from hourly precipitation (Pr) data for each grid cell. Quantile-quantile plot (b) for BC and FC for different land covers. Land area is defined as non-sea and non-urban areas in the domain of interest. Like PDFs, quantile values are the average of individual grid cell values. (c) PDFs of area-averaged temperature for three scenarios (BC and two FCs) for the entire domain, sea, land and city. (d) The FC-BC difference for sea, land, and city (upper subpanel); the FC-BC difference after Clausius-Clapeyron (CC) scaling (assuming a humidity increase of 7% per K warming). Uncertainty ranges shown in all panels indicate annual variability, that is, the range between percentile 25 and 75 of annual values (10 years).

In addition to the frequency, the changes in intensity are essential because of their urban flood implications. An interesting trend is seen as the more substantial intensification is likely to happen at upper-quantile precipitations. For example, with RCP8.5, precipitation of quantiles 0.95 and 0.99 are anticipated to increase by 3.3 and 5.8 mm/hr from 18.9 to 33.4 mm/hr in the present climate, corresponding to increases of 17.4% and 17.6%, respectively, for the land area. Also, the intensity change shows it is RCP scenario dependent (Figures 2a and 2d). The absolute increase of quantile 0.95 and 0.99 for RCP8.5 is roughly double that for RCP4.5. Further, while it varies among land, sea, and city, the variation is relatively small compared to inter-scenario differences. Nevertheless, precipitation intensification is highest over water, followed by land area and most minor changes over the city (Figure 2d).

Assessing the precipitation changes by taking the CC and rainfall change relation ( $\sim 7\%$  for 1K warming) as a reference can help provide an insightful understanding about the climatic response (Fowler, Ali, et al., 2021; Fowler, Lenderink, et al., 2021). It is interesting to note that despite variations in absolute values (Figure 2d left panel), changes in rainfall intensities are likely to converge regardless of the RCP scenario. The asymmetric trend is seen among different quantiles (Figure 2d right panel). The upper quantiles show more remarkable changes in terms of the CC rate. Over the sea, the change rate even exceeds 1.0, that is, the “super” CC rate. Together with the changes in precipitation frequency, a consistent finding emerges: the heavier the current precipitation is, the more intense and frequent it will be in the future. For less heavy rainfall, the changes are expected to be minor and insignificant.

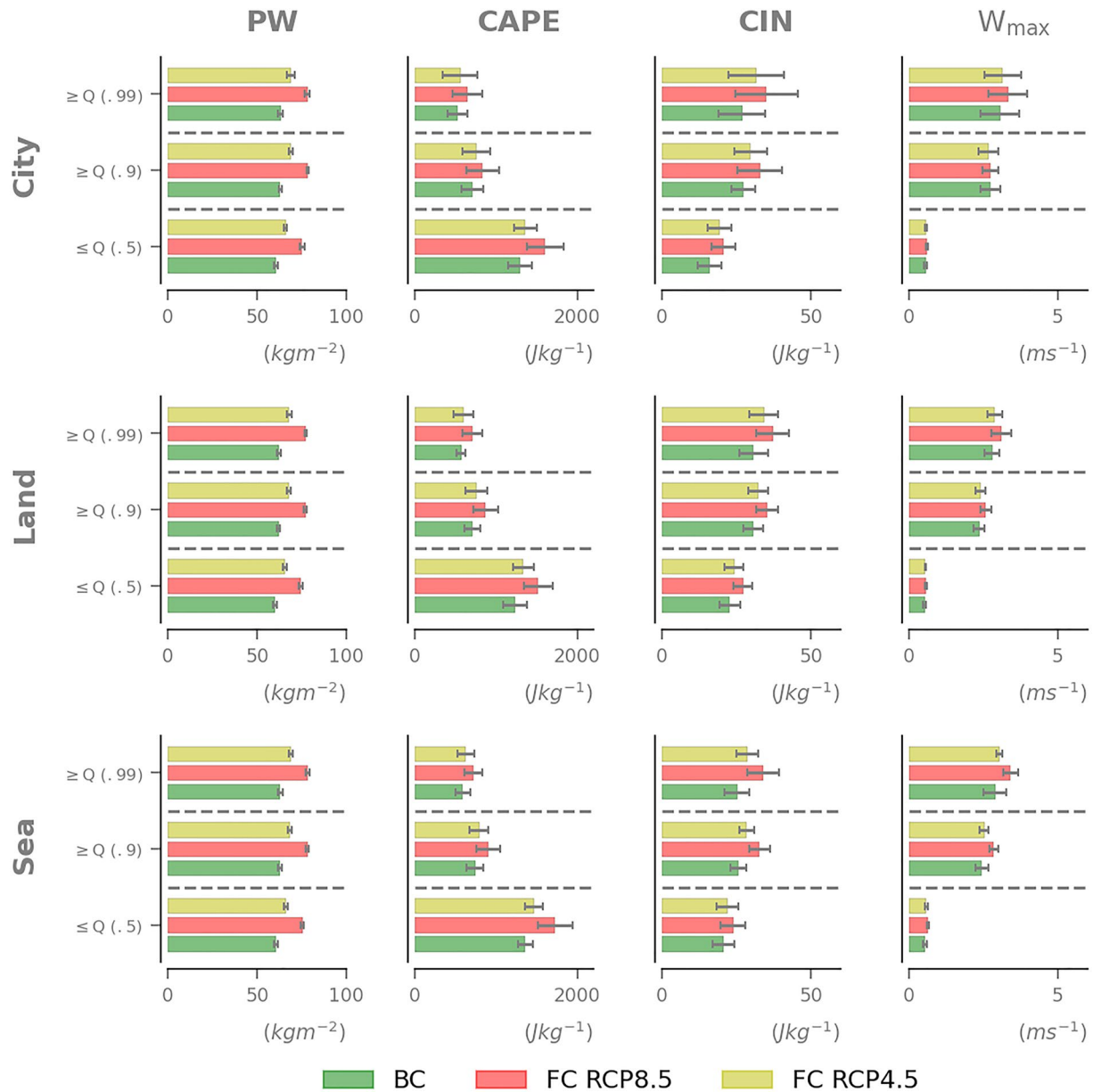


**Figure 3.** Change in atmospheric variables associated with precipitation. Shown are from top to bottom precipitable water (PW), convective available potential energy (CAPE), convective inhibition (CIN), and maximum vertical velocity ( $W_{max}$ ) for three different land covers (left to right) and for three precipitation types, that is, below quantile 0.5, above quantile 0.9, and 0.99. Values are area averages for the respective land covers. Different bar color indicates values of baseline climate (BC), and future climates with two RCP scenarios (FC RCP8.5, and RCP4.5). Uncertainty ranges shown in all panels indicate annual variability, that is, the range between percentile 25 and 75 of annual values (10 years).

The increase in future precipitation generally and especially in extremes is attributed to two possible factors if excluding the impacts of aerosol. The first is an increase in atmospheric moisture (the “fuel” for convective potential). The second is an enhanced vertical motion that lifts low-level moisture upward and favors more vigorous convection and more precipitation. The change in the atmospheric moisture is analyzed by examining the differences in total precipitable water between FC and BC (PW, Figure 3). For example, FC RCP8.5 exhibits a 14 mm, or approximately 24%, increase compared to BC. A weaker increase is noted under FC RCP4.5. This trend is similar across sea, land, city, and precipitation types, that is, moderate and heavy.

On the other hand, the changes in convective available potential energy (CAPE) and convective inhibition (CIN) vary among precipitation types and land covers. CAPE is a widely used measure that indicates atmospheric



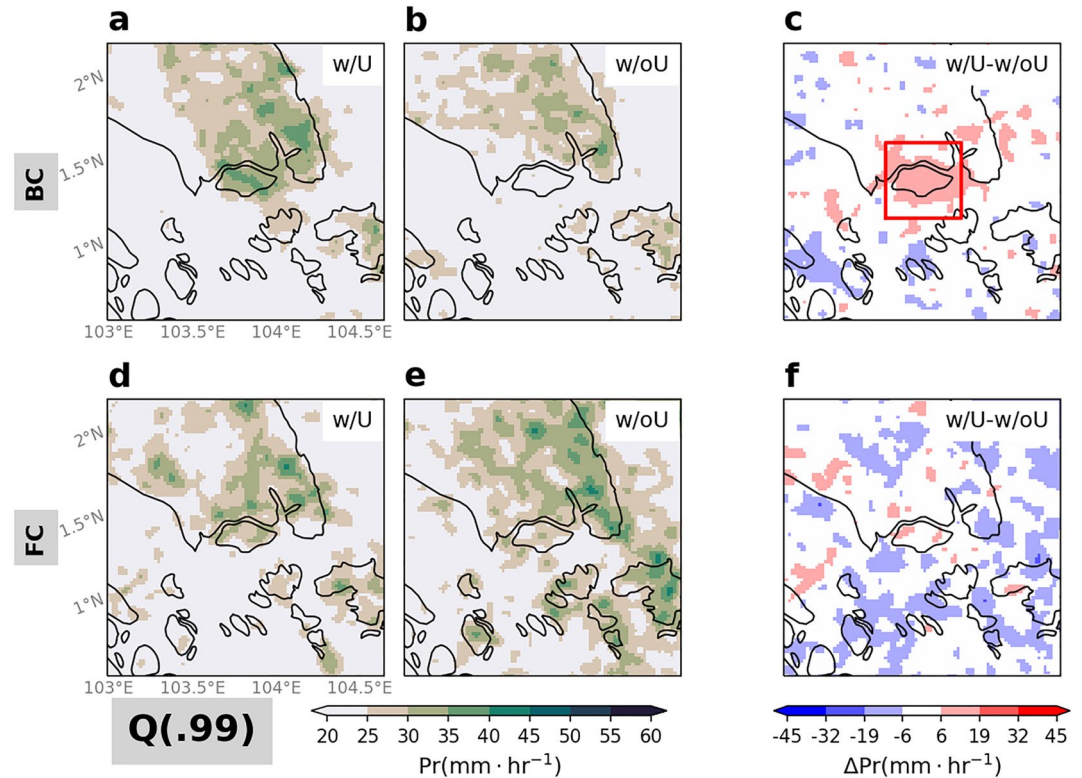


**Figure 4.** Spatial distribution of precipitation (Pr) of quantile 0.99 [Q(0.99)]. (a, b) Results from baseline climate (BC) simulations with and (w/U) without urban land use/cover (w/oU) and (c) the difference between them (w/U – w/oU). (d, e, f) The same as (a, b, c) but for future climate (FC) assuming scenario RCP8.5. Quantile values were calculated based on hourly accumulated rainfall data, 12–18 p.m., each day, November 2005–2014. Red rectangle in (c) indicates the area of Singapore and its neighbor city, Johor Bahru.

instability and a necessary condition for generating convection. CAPE may provide insight on how “convective” precipitation extremes are (Barbero et al., 2019). In contrast, CIN indicates suppression of convection development, which inhibits air parcels from rising from the surface to the level of free convection. Not surprisingly, results revealed a noticeable increase in CAPE in the future (up to 30%–40% with RCP8.5), indicating that a warmer atmosphere will provide a more favorable environment for convection (CAPE, Figure 3). However, CIN also shows an increasing trend, meaning that the “negative” force to suppress convection development is enhanced (CIN, Figure 3). Note that increased CIN temporarily inhibits convection allowing CAPE to rise further. Thus, when convection does trigger, it becomes more intense (Emanuel, 1994; Stull, 2016). One interesting fact worthy to note is that higher CAPE and lower CIN trends are seen for light precipitation (lower than quantile 0.5) compared to EP (higher than quantile 0.9, 0.99). Results for lifting force, in terms of maximum vertical wind speed ( $W_{max}$ ), provide a different insight. Overall,  $W_{max}$  with light precipitation is very small compared to EP ( $W_{max}$ , Figure 3). On the other hand,  $W_{max}$  during heavy and EP is very high ( $\sim 3$  m/s), and further increases in the future. This result implies that the change in lifting force, in addition to CAPE, might play a more critical role in the story of EP. Indeed, the diurnal cycle of rainfall for different thresholds (Figure S4 in Supporting Information S1) shows a decrease in the frequency of EP over the land area, particularly in the afternoon despite CAPE being highest.

Further questions are (a) how does the urban area impact precipitation extreme events? (b) how will this impact change under warmer climates? To answer these, first, we compare the results of BCw/U to BCw/oU (i.e., the baseline-climate simulations with and without urban land use/cover). The results show that BCw/U consistently produced significantly higher precipitation over the urban area than BCw/oU, especially during the afternoon when the urban effect on convection is likely strongest. In the other words, the “urban wet island” (UWI) effect was well reproduced by the model. For example, Figure 4 shows that BCw/U produced higher precipitation, by about  $10 \text{ mm} \cdot \text{hr}^{-1}$ , over the urban area than BCw/oU, for Q(0.99); quantile 0.99; Figures 4a–4c). The UWI effect

is visible for other quantiles as well, such as 0.9 and 0.5, though it disappears at  $Q(0.1)$ ; see Figures S5–S7 in Supporting Information S1). The detected urban impact is in line with previous studies over Singapore by Doan et al. (2021) and Simón-Moral et al. (2021), which used a different numerical model (UK's Unified Model) investigating different aspects of urban precipitation (the climate mean). Both Doan and Simon-Moral et al. concluded that the urban precipitation enhancement over Singapore is attributed to the UHI effect, which destabilizes the low-level atmosphere and encourages horizontal moisture convergence. These mechanisms are also confirmed in our results (not shown).

Investigating different climate regimes, comparison between FCw/U and FCw/oU (future climate simulations with and without urban land use/cover) revealed that the UWI effect confirmed in BC simulations is no longer apparent in FC simulations. The FCw/U—FCw/oU difference does not show a clear UWI (Figures 4d–4f) when compared to BCw/U—BCw/oU. There are still visible differences between the two simulations, however, they seem randomly distributed and not directly connected with the spatial form of the city. This trend consistently appears for other precipitation quantiles, that is, 0.9, 0.5, 0.1 (Figures S5–S7 in Supporting Information S1).

The above result highlights the possibility that global warming could modify and even reduce the urban footprint on EP events. More evidence, however, is needed to make general conclusions given that the present simulations include only a particular city. Several possible mechanisms are investigated to explain this result. The BC and FC simulations do not show a notable difference in the UHI in terms of surface air temperature (Figure S8 in Supporting Information S1). Thus, even though the UHI does not show major alterations, the static-stability and convection-related variables such as CAPE and CIN in the model show a difference between BC and FC runs (as shown in Figures 3 and S9 in Supporting Information S1). It is likely that CIN increases to a level that may suppress urban-enhanced convections. Another possible precipitation-reducing mechanism includes changes in the sea breeze regime (as a local convection trigger) in a warming climate. This could be particularly important in the case of Singapore, given its coastal location.

#### 4. Conclusions

For the first time, this study demonstrates the global-warming-induced substantial enhancement of extreme hourly precipitation in terms of both intensity and frequency over a tropical urban agglomeration, Singapore, based on simulation results with the convection-permitting WRF model. Interestingly, the enhancement is not uniform among precipitation at different intensities, given the same increasing rate of atmospheric water vapor. The more EP is intensified further in the future warming environment. Notably, an intensified rate of very extreme events (greater than quantile 0.99) can reach a “super” CC rate (greater than +7% per K). In contrast, the intensification of moderate and light precipitation (lower than quantile 0.5) is lower and close to zero CC rate. This new normal can be expressed as “extreme events get more extreme.” The result is significant for urban planners. The asymmetric nature of the future enhancement of precipitation has to be considered in mitigating more severe urban flash flooding caused by increased intense precipitation events. This is especially important for coastal cities over the low-latitude tropical area, where sea-level rise, another impact of global warming, is more serious (Spada et al., 2013).

Our study highlights the possibility that global warming could modify and even reduce the urban footprint on precipitation extreme events, especially during the afternoon when the urban impact on convection is likely strongest. The “urban wet island” effect, which is obvious under the baseline climate, will no longer be apparent under the warmer climate regime. The possible explanation for this is enhanced atmospheric stratification in terms of increased CIN works to dampen urban-boosted convection to form. More evidence, however, is needed to generalize the conclusions, given that the present simulations include only one particular city.

Several uncertainties remain in this study. First, as we isolate the primary thermodynamic signal of global warming by employing the PGW approach for dynamical downscaling, we ignore secondary signals such as potential changes in inter-annual variabilities or changes in large-scale weather patterns which could influence the EP climate. However, comprehensively including global warming impacts in the sense of direct dynamical downscaling could blur the first signal of global warming on localized precipitation, making it difficult to derive a clear conclusion. We also do not discuss the model's uncertainty related to future changes in urban surface conditions or the impact of aerosols.

## Data Availability Statement

The source code of WRF model Version 3.5.1 used in this study can be downloaded from [https://www2.mmm.ucar.edu/wrf/users/download/get\\_sources.html](https://www2.mmm.ucar.edu/wrf/users/download/get_sources.html). The ERA-Interim reanalysis data used as initial/boundary conditions for the WRF model is openly available in <https://www.ecmwf.int/en/forecasts/datasets/reanalysis-datasets/era-interim>. The urban land use/cover data used for the simulations are provided by the World Urban Database project <http://www.wudapt.org/cities/in-asia/>.

## Acknowledgments

This research is funded by JSPS KAKENHI Grant Nos. 20K13258; JSPS KAKENHI Grant Nos. 19H01155; NASA IDS Grant # 80NSSC20K1262; USDA NIFA Grants 2015-67003-23460. Numerical calculations were performed using Oakforest-PACS system under the Multidisciplinary Cooperative Research Program at the Center for Computational Sciences, University of Tsukuba.

## References

- Ali, H., Fowler, H. J., Lenderink, G., Lewis, E., & Pritchard, D. (2021). Consistent large-scale response of hourly extreme precipitation to temperature variation over land. *Geophysical Research Letters*, *48*(4), e2020GL090317. <https://doi.org/10.1029/2020GL090317>
- Ali, H., & Mishra, V. (2018). Increase in subdaily precipitation extremes in India under 1.5 and 2.0°C warming worlds. *Geophysical Research Letters*, *45*(14), 6972–6982. <https://doi.org/10.1029/2018GL078689>
- Ali, H., Peleg, N., & Fowler, H. J. (2021). Global scaling of rainfall with dewpoint temperature reveals considerable ocean-land difference. *Geophysical Research Letters*, *48*(15), e2021GL093798. <https://doi.org/10.1029/2021GL093798>
- Allan, R. P., & Soden, B. J. (2008). Atmospheric warming and the amplification of precipitation extremes. *Science*, *321*(5895), 1481–1484. <https://doi.org/10.1126/science.1160787>
- Barbero, R., Fowler, H. J., Blenkinsop, S., Westra, S., Moron, V., Lewis, E., et al. (2019). A synthesis of hourly and daily precipitation extremes in different climatic regions. *Weather and Climate Extremes*, *26*, 100219. <https://doi.org/10.1016/j.wace.2019.100219>
- Berg, P., Moseley, C., & Haerter, J. O. (2013). Strong increase in convective precipitation in response to higher temperatures. *Nature Geoscience*, *6*(3), 181–185. <https://doi.org/10.1038/ngeo1731>
- Bornstein, R., Thunis, P., & Schayes, G. (1994). Observation and simulation of urban-topography barrier effects on boundary layer structure using the three-dimensional TVM/URBEMET model. In S.-E. Gryning, & M. M. Millán (Eds.), *Air pollution modeling and its application X* (pp. 101–108). Springer US. [https://doi.org/10.1007/978-1-4615-1817-4\\_12](https://doi.org/10.1007/978-1-4615-1817-4_12)
- Chen, F., Miao, S., Mukul, T., Bao, J. W., & Kusaka, H. (2011). A numerical study of interactions between surface forcing and sea breeze circulations and their effects on stagnation in the greater Houston area. *Journal of Geophysical Research*, *116*(D12), D12105. <https://doi.org/10.1029/2010jd015533>
- Dee, D. P., Uppala, S. M., Simmons, A. J., Berrisford, P., Poli, P., Kobayashi, S., et al. (2011). The ERA-interim reanalysis: Configuration and performance of the data assimilation system. *Quarterly Journal of the Royal Meteorological Society*, *137*(656), 553–597. <https://doi.org/10.1002/qj.828>
- Demuzere, M., Kittner, J., & Bechtel, B. (2021). LCZ generator: A web application to create local climate zone maps. *Frontiers in Environmental Science*, *9*. <https://doi.org/10.3389/fenvs.2021.637455>
- Deser, C., Phillips, A., Bourdette, V., & Teng, H. (2012). Uncertainty in climate change projections: The role of internal variability. *Climate Dynamics*, *38*(3), 527–546. <https://doi.org/10.1007/s00382-010-0977-x>
- Diffenbaugh, N. S., Singh, D., Mankin, J. S., Horton, D. E., Swain, D. L., Touma, D., et al. (2017). Quantifying the influence of global warming on unprecedented extreme climate events. *Proceedings of the National Academy of Sciences*, *114*(19), 4881–4886. <https://doi.org/10.1073/pnas.1618082114>
- Doan, Q.-V., Dipankar, A., Simón-Moral, A., Sanchez, C., Prasanna, V., Roth, M., & Huang, X.-Y. (2021). Urban-induced modifications to the diurnal cycle of rainfall over a tropical city. *Quarterly Journal of the Royal Meteorological Society*, *147*(735), 1189–1201. <https://doi.org/10.1002/qj.3966>
- Doan, Q.-V., & Kusaka, H. (2018). Projections of urban climate in the 2050s in a fast-growing city in Southeast Asia: The greater Ho Chi Minh City metropolitan area, Vietnam. *International Journal of Climatology*, *38*(11), 4155–4171. <https://doi.org/10.1002/joc.5559>
- Dudhia, J. (1989). Numerical study of convection observed during the winter monsoon experiment using a mesoscale two-dimensional model. *Journal of the Atmospheric Sciences*, *46*(20), 3077–3107. [https://doi.org/10.1175/1520-0469\(1989\)046<3077:NSOCOD>2.0.CO;2](https://doi.org/10.1175/1520-0469(1989)046<3077:NSOCOD>2.0.CO;2)
- Emanuel, K. A. (1994). *Atmospheric convection* (1st ed.). Oxford University Press.
- Fischer, E. M., & Knutti, R. (2016). Observed heavy precipitation increase confirms theory and early models. *Nature Climate Change*, *6*(11), 986–991. <https://doi.org/10.1038/nclimate3110>
- Fischer, E. M., Sippel, S., & Knutti, R. (2021). Increasing probability of record-shattering climate extremes. *Nature Climate Change*, *11*(8), 689–695. <https://doi.org/10.1038/s41558-021-01092-9>
- Fong, M., & Ng, L. K. (2012). *The weather and climate of Singapore*. Meteorological Service Singapore.
- Fowler, H. J., Ali, H., Allan, R. P., Ban, N., Barbero, R., Berg, P., et al. (2021). Towards advancing scientific knowledge of climate change impacts on short-duration rainfall extremes. *Philosophical Transactions of the Royal Society A: Mathematical, Physical & Engineering Sciences*, *379*(2195), 20190542. <https://doi.org/10.1098/rsta.2019.0542>
- Fowler, H. J., Lenderink, G., Prein, A. F., Westra, S., Allan, R. P., Ban, N., et al. (2021). Anthropogenic intensification of short-duration rainfall extremes. *Nature Reviews Earth & Environment*, *2*(2), 107–122. <https://doi.org/10.1038/s43017-020-00128-6>
- Guerreiro, S. B., Fowler, H. J., Barbero, R., Westra, S., Lenderink, G., Blenkinsop, S., et al. (2018). Detection of continental-scale intensification of hourly rainfall extremes. *Nature Climate Change*, *8*(9), 803–807. <https://doi.org/10.1038/s41558-018-0245-3>
- Gutmann, E. D., Rasmussen, R. M., Liu, C., Ikeda, K., Bruyere, C. L., Done, J. M., et al. (2018). Changes in hurricanes from a 13-yr convection-permitting pseudo-global warming simulation. *Journal of Climate*, *31*(9), 3643–3657. <https://doi.org/10.1175/JCLI-D-17-0391.1>
- Hamdi, R., Kusaka, H., Doan, Q.-V., Cai, P., He, H., Luo, G., et al. (2020). The state-of-the-art of urban climate change modeling and observations. *Earth Systems and Environment*, *4*(4), 631–646. <https://doi.org/10.1007/s41748-020-00193-3>
- Heever, S. C. v. d., & Cotton, W. R. (2007). Urban aerosol impacts on downwind convective storms. *Journal of Applied Meteorology and Climatology*, *46*(6), 828–850. <https://doi.org/10.1175/JAM2492.1>
- Hibino, K., Takayabu, I., Wakazuki, Y., & Ogata, T. (2018). Physical responses of convective heavy rainfall to future warming condition: Case study of the Hiroshima event. *Frontiers of Earth Science*, *6*, 35. <https://doi.org/10.3389/feart.2018.00035>
- Hong, S.-Y. (2006). Hongandlim-JKMS-2006. *Journal of the Korean Meteorological Society*, *42*, 129–151.
- Hong, S.-Y., Noh, Y., & Dudhia, J. (2006). A new vertical diffusion package with an explicit treatment of entrainment processes. *Monthly Weather Review*, *134*(9), 2318–2341. <https://doi.org/10.1175/MWR3199.1>

- IPCC AR6. (2022). *AR6 synthesis report: Climate change 2022—IPCC*. Retrieved from <https://www.ipcc.ch/report/sixth-assessment-report-cycle/>
- Joyce, R. J., Janowiak, J. E., Arkin, P. A., & Xie, P. (2004). CMORPH: A method that produces global precipitation estimates from passive microwave and infrared data at high spatial and temporal resolution. *Journal of Hydrometeorology*, 5(3), 487–503. [https://doi.org/10.1175/1525-7541\(2004\)005<0487:CAMTPG>2.0.CO;2](https://doi.org/10.1175/1525-7541(2004)005<0487:CAMTPG>2.0.CO;2)
- Kain, J. S. (2004). The Kain–Fritsch convective parameterization: An update. *Journal of Applied Meteorology and Climatology*, 43(1), 1702–2181. [https://doi.org/10.1175/1520-0450\(2004\)043<0170:TKCPAU>2.0](https://doi.org/10.1175/1520-0450(2004)043<0170:TKCPAU>2.0)
- Kishtawal, C. M., Niyogi, D., Tewari, M., Pielke Sr, R. A., & Shepherd, J. M. (2010). Urbanization signature in the observed heavy rainfall climatology over India. *International Journal of Climatology*, 30(13), 1908–1916.
- Kusaka, H., & Kimura, F. (2004). Coupling a single-layer urban canopy model with a simple atmospheric model: Impact on urban heat island simulation for an idealized case. *Journal of the Meteorological Society of Japan*, 82(1), 67–80. <https://doi.org/10.2151/jmsj.82.67>
- Kusaka, H., Kondo, H., Kikegawa, Y., & Kimura, F. (2001). A simple single-layer urban canopy model for atmospheric models: Comparison with multi-layer and slab models. *Boundary-Layer Meteorology*, 101(3), 329–358. <https://doi.org/10.1023/A:1019207923078>
- Kusaka, H., Nawata, K., Suzuki-Parker, A., Takane, Y., & Furuhashi, N. (2014). Mechanism of precipitation increase with urbanization in Tokyo as revealed by ensemble climate simulations. *Journal of Applied Meteorology and Climatology*, 53(4), 824–839.
- Lauer, A., Zhang, C., Elison-Timm, O., Wang, Y., & Hamilton, K. (2013). Downscaling of climate change in the Hawaii region using CMIP5 results: On the choice of the forcing fields. *Journal of Climate*, 26(24), 10006–10030. <https://doi.org/10.1175/JCLI-D-13-00126.1>
- Lenderink, G., & Meijgaard, E. v. (2010). Linking increases in hourly precipitation extremes to atmospheric temperature and moisture changes. *Environmental Research Letters*, 5(2), 025208. <https://doi.org/10.1088/1748-9326/5/2/025208>
- Lenderink, G., & van Meijgaard, E. (2009). Unexpected rise in extreme precipitation caused by a shift in rain type? *Nature Geoscience*, 2(6), 373. <https://doi.org/10.1038/ngeo524>
- Li, Y., Fowler, H. J., Argüeso, D., Blenkinsop, S., Evans, J. P., Lenderink, G., et al. (2020). Strong intensification of hourly rainfall extremes by urbanization. *Geophysical Research Letters*, 47(14), e2020GL088758. <https://doi.org/10.1029/2020GL088758>
- Liu, J., & Niyogi, D. (2019). Meta-analysis of urbanization impact on rainfall modification. *Scientific Reports*, 9(1), 7301. <https://doi.org/10.1038/s41598-019-42494-2>
- Meehl, G. A., Goddard, L., Murphy, J., Stouffer, R. J., Boer, G., Danabasoglu, G., et al. (2009). Decadal prediction: Can it be skillful? *Bulletin of the American Meteorological Society*, 90(10), 1467–1486. <https://doi.org/10.1175/2009BAMS2778.1>
- Meyer, L., Brinkman, S., van Kesteren, L., Leprince-Ringuet, N., & van Boxmeer, F. (2020). *Technical support unit for the synthesis report* (Vol. 169).
- Mishra, A., Mukherjee, S., Merz, B., Singh, V. P., Wright, D. B., Villarini, G., et al. (2022). An Overview of Flood Concepts, Challenges, and Future Directions. *Journal of Hydrologic Engineering*, 27(6), 03122001.
- Mlawer, E. J., Taubman, S. J., Brown, P. D., Iacono, M. J., & Clough, S. A. (1997). Radiative transfer for inhomogeneous atmospheres: RRTM, a validated correlated-k model for the longwave. *Journal of Geophysical Research*, 102(D14), 16663–16682. <https://doi.org/10.1029/97JD00237>
- Moustakis, Y., Onof, C. J., & Paschalis, A. (2020). Atmospheric convection, dynamics and topography shape the scaling pattern of hourly rainfall extremes with temperature globally. *Communications Earth & Environment*, 1(1), 1–9. <https://doi.org/10.1038/s43247-020-0003-0>
- Mukul Tewari, N., Tewari, M., Chen, F., Wang, W., Dudhia, J., LeMone, M., et al. (2004). Implementation and verification of the unified NOAA land surface model in the WRF model. *Presented at the 20th conference on weather analysis and forecasting/16th conference on numerical weather prediction* (Formerly Paper Number 17.5) (pp. 11–15).
- NCEP. (2021). *NOAA climate data record (CDR) of CPC morphing technique (CMORPH) high resolution global precipitation estimates*. Retrieved from <https://www.nci.noaa.gov/access/metadata/landing-page/bin/iso?id=gov.noaa.ncdc:C00948>
- Niyogi, D., Pyle, P., Lei, M., Arya, S. P., Kishtawal, C. M., Shepherd, M., et al. (2011). Urban modification of thunderstorms: An observational storm climatology and model case study for the Indianapolis urban region. *Journal of Applied Meteorology and Climatology*, 50(5), 1129–1144.
- Pall, P., Patricola, C. M., Wehner, M. F., Stone, D. A., Paciorek, C. J., & Collins, W. D. (2017). Diagnosing conditional anthropogenic contributions to heavy Colorado rainfall in September 2013. *Weather and Climate Extremes*, 17, 1–6. <https://doi.org/10.1016/j.wace.2017.03.004>
- Panthou, G., Mailhot, A., Laurence, E., & Talbot, G. (2014). Relationship between surface temperature and extreme rainfalls: A multi-time-scale and event-based analysis. *Journal of Hydrometeorology*, 15(5), 1999–2011. <https://doi.org/10.1175/JHM-D-14-0020.1>
- Park, I.-H., & Min, S.-K. (2017). Role of convective precipitation in the relationship between subdaily extreme precipitation and temperature. *Journal of Climate*, 30(23), 9527–9537. <https://doi.org/10.1175/JCLI-D-17-0075.1>
- Rajczak, J., & Schär, C. (2017). Projections of future precipitation extremes over Europe: A multimodel assessment of climate simulations. *Journal of Geophysical Research: Atmospheres*, 122(2010), 773–810. <https://doi.org/10.1002/2017JD027176>
- Rasmussen, R., Liu, C., Ikeda, K., Gochis, D., Yates, D., Chen, F., et al. (2011). High-resolution coupled climate runoff simulations of seasonal snowfall over Colorado: A process study of current and warmer climate. *Journal of Climate*, 24(12), 3015–3048. <https://doi.org/10.1175/2010JCLI3985.1>
- Sato, T., Kimura, F., & Kitoh, A. (2007). Projection of global warming onto regional precipitation over Mongolia using a regional climate model. *Journal of Hydrology*, 333(1), 144–154. <https://doi.org/10.1016/j.jhydrol.2006.07.023>
- Schär, C., Frei, C., Lüthi, D., & Davies, H. C. (1996). Surrogate climate-change scenarios for regional climate models. *Geophysical Research Letters*, 23(6), 669–672. <https://doi.org/10.1029/96GL00265>
- Scherrer, S. C., Fischer, E. M., Posselt, R., Liniger, M. A., Croci-Maspoli, M., & Knutti, R. (2016). Emerging trends in heavy precipitation and hot temperature extremes in Switzerland. *Journal of Geophysical Research: Atmospheres*, 121(6), 2626–2637. <https://doi.org/10.1002/2015JD024634>
- Shem, W., & Shepherd, M. (2009). On the impact of urbanization on summertime thunderstorms in Atlanta: Two numerical model case studies. *Atmospheric Research*, 92(2), 172–189. <https://doi.org/10.1016/j.atmosres.2008.09.013>
- Shepherd, T. G. (2014). Atmospheric circulation as a source of uncertainty in climate change projections. *Nature Geoscience*, 7(10), 703–708. <https://doi.org/10.1038/ngeo2253>
- Simón-Moral, A., Dipankar, A., Doan, Q.-V., Sanchez, C., Roth, M., Becker, E., & Huang, X.-Y. (2021). Urban intensification of convective rainfall over the Singapore—Johor Bahru region. *Quarterly Journal of the Royal Meteorological Society*. <https://doi.org/10.1002/qj.4147>
- Singh, J., Karmakar, S., PaiMazumder, D., Ghosh, S., & Niyogi, D. (2020). Urbanization alters rainfall extremes over the contiguous United States. *Environmental Research Letters*, 15(7), 074033.
- Skamarock, W. C., Klemp, J. B., Dudhia, J., Gill, D. O., Barker, D., Duda, M. G., et al. (2008). *A description of the advanced research WRF version 3*. NCAR technical notes, NCAR/TN-4751STR.
- Spada, G., Bamber, J. L., & Hurkmans, R. T. W. L. (2013). The gravitationally consistent sea-level fingerprint of future terrestrial ice loss. *Geophysical Research Letters*, 40(3), 482–486. <https://doi.org/10.1029/2012GL053000>

- Stull, R. (2016). *Practical meteorology: An algebra-based Survey of atmospheric science* (black and white ed.). Sundog Publishing, LLC.
- Taylor, K. E., Stouffer, R. J., & Meehl, G. A. (2012). An overview of CMIP5 and the experiment design. *Bulletin of the American Meteorological Society*, 93(4), 485–498. <https://doi.org/10.1175/BAMS-D-11-00094.1>
- United Nations (2015). *Sustainable development goals*. Retrieved from <https://www.undp.org/sustainable-development-goals>
- van Vuuren, D. P., Edmonds, J. A., Kainuma, M., Riahi, K., & Weyant, J. (2011). A special issue on the RCPs. *Climatic Change*, 109(1–2), 1–4. <https://doi.org/10.1007/s10584-011-0157-y>
- Wang, J., Chen, F., Doan, Q.-V., & Xu, Y. (2021). Exploring the effect of urbanization on hourly extreme rainfall over Yangtze River Delta of China. *Urban Climate*, 36, 100781. <https://doi.org/10.1016/j.uclim.2021.100781>
- Wasko, C., Parinussa, R. M., & Sharma, A. (2016). A quasi-global assessment of changes in remotely sensed rainfall extremes with temperature. *Geophysical Research Letters*, 43(2412), 659668–659712. <https://doi.org/10.1002/2016GL071354>
- Westra, S., Fowler, H. J., Evans, J. P., Alexander, L. V., Berg, P., Johnson, F., et al. (2014). Future changes to the intensity and frequency of short-duration extreme rainfall. *Reviews of Geophysics*, 52(3), 522–555. <https://doi.org/10.1002/2014RG000464>
- Yang, L., Ni, G., Tian, F., & Niyogi, D. (2021). Urbanization Exacerbated Rainfall over European Suburbs under a Warming Climate. *Geophysical Research Letters*, 48(21), e2021GL095987.
- Ye, X., & Niyogi, D. (2022). Resilience of human settlements to climate change needs the convergence of urban planning and urban climate science. *Computational Urban Science*, 2(1), 1–4.